Effect of Gas Impurities on the Throttling Process of Fluorocarbon Refrigerants: Estimation of the Henry's Law Constant†

Václav Vinš*,‡,§ and Václav Vacek‡

Faculty of Mechanical Engineering, Czech Technical University in Prague, Technická 4, 16607 Prague 6, Czech Republic, and Institute of Thermomechanics AS ČR, v.v.i., Dolejškova 1402, 18200 Prague 8, Czech Republic

The effect of the presence of noncondensing gases on the throttling process of a saturated fluorocarbon refrigerant was studied. Two-phase flow of the throttled refrigerant was investigated in a special divided small-diameter tube equipped with pressure and temperature sensors. Gas impurities affected the manner of onset of vaporization and consequently decreased the overall effectiveness of a vapor cooling circuit. Available literature data on three gases (O_2, Xe, N_2) was collected and analyzed to establish a simple temperature correlation for the Henry's law constant of gases dissolved in saturated fluorocarbons at a low gas partial pressure around 0.1 MPa. The Peng-Robinson cubic equation of state and the perturbed-chain modification of statistical associating fluid theory (PC-SAFT) were employed to predict the temperature dependency of gas solubility in fluorinert substances.

Introduction

Saturated fluorocarbons, also known as fluorinert liquids, are used as solvents, anticorrosive components, refrigerants, and, for their high gas solubility, even as blood substitutes. Due to their dielectric performance, radiation hardness, e.g., resistance to radiation damage, and chemical stability, perfluoropropane (n-C_3F_8, refrigerant R218) and perfluorobutane (n-C_4F_{10}, refrigerant R610) are two components that are employed for cooling electronic equipment for particle detectors built at the CERN laboratory.[1] Great attention has been dedicated to investigating the throttling process and the two-phase flow of fluorocarbon refrigerant in small-bore tubes (capillary tubes).[2−4] The character of the refrigerant flow in such tubes, used as expansion devices, significantly affects the overall performance of the whole cooling circuit.

Many researchers have presented studies of the throttling process within a capillary tube of standard refrigerants such as R12, R22, R134a, and R600a and of refrigerant mixtures R407c and R410a, especially during the last 15 years. Several quite complex models have been prepared for refrigerant flow through small-diameter tubes, based mostly on a numerical solution of the governing equations of single-phase and two-phase flow of a vapor−liquid mixture.[5,6] Some of these simulations even allow us to predict the behavior of a nonadiabatic refrigerant flow and do not just offer a simplified model of the more common case of an adiabatic flow.[7,8] The accuracy of the models is relatively good and is in most cases adequate. Most of the models predicting the performance of the capillary tube were verified on rather limited or replicated sets of experimental data from the literature, which at least provided good information on the pressure and temperature profile within capillary tubes. Unfortunately, there have only been a limited number of experimental studies presenting the precise behavior of a throttled refrigerant within a capillary tube. Moreover, most of these measurements have been performed with obsolete refrigerants such as R12 and not with refrigerant substitutes of present interest. In addition, the various experimental data sets show some discrepancies, most probably caused by refrigerant oil contamination or by other effects. All such deficiencies can complicate the verification process of theoretical models of throttling inside a capillary tube. Some researchers have already focused their attention on these impacts. For example, Huerta et al.[9] recently presented a detailed experimental study of R134a capillary flow under clean and oil-contaminated conditions.

We have performed an experimental investigation of the throttling process of several saturated fluorocarbons using a model capillary tube that was produced in house. Large amounts of data were also collected during capillary tuning and trimming for real cooling circuits with complex manifolding with as many as 200 different cooling loops. The measurements provide detailed information about the flow behavior of clean refrigerant n-C_3F_8 throttled in small-bore tube. However, we also detected a quite significant effect of noncondensing gas impurities affecting the pattern of the two-phase flow during our experimental tests.

We are at present working on a theoretical description and prediction of this effect for perfluoropropane. Solubility of gases in liquids is described by Henry's law, which defines the relation between the solute (gas) partial pressure and the mole fraction of gas dissolved in a liquid solvent. Since the pressure drop of a boiling refrigerant during the throttling process is accompanied by a sharp temperature drop, knowledge of the correct value of the Henry's law constant and especially of its temperature dependency is required.

This report summarizes available experimental data on the solubility of common gases collected from the literature, namely, oxygen, xenon, and nitrogen, in fluorinert liquids. Simple correlations of the Henry's law constant for heavy fluorinerts were determined on the basis of literature data. The main motivation of this project was to prepare the temperature correlation of the Henry's law constant for nitrogen dissolved

* Corresponding author. Phone: +420 608 51 41 06. Fax: +420 286 584 695. E-mail: vins.vaclav@seznam.cz.
† Part of the "William A. Wakeham Festschrift".
‡ Czech Technical University in Prague.
§ Institute of Thermomechanics AS ČR.

10.1021/je800819h CCC: $40.75
Published on Web 03/02/2009

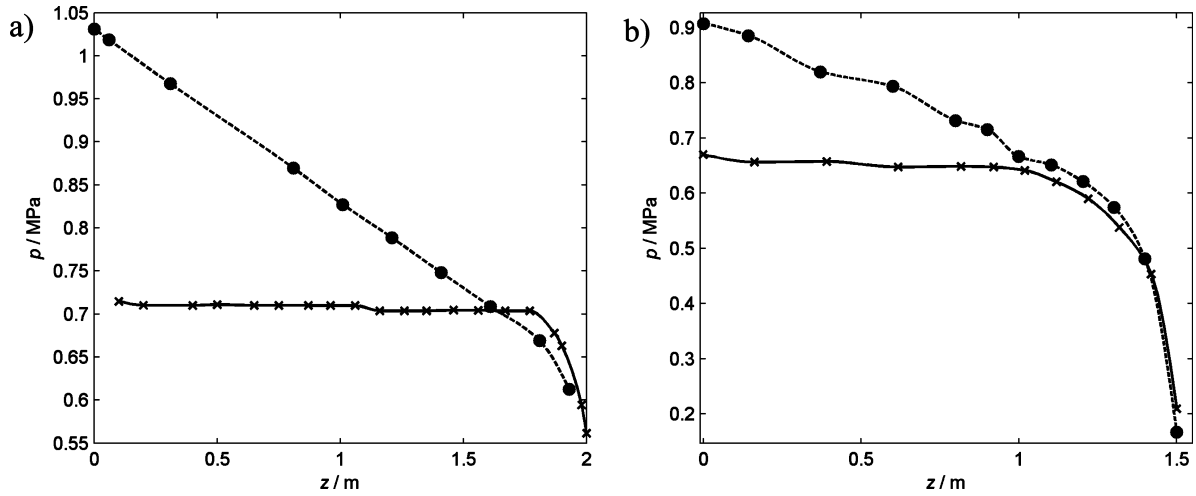

Figure 1. Variation of: -●-, pressure; -×-, saturation pressure determined from measured temperature. Experimental data of R134a presented by other authors. (a) Huerta[9] data of clean refrigerant flow measured on capillary tube with inner diameter ID = 0.82 mm, subcooled liquid temperature at capillary tube inlet T_{in} = 300.4 K, and refrigerant mass flow rate $\dot{m}$ = 2.186 g·s^{-1}. (b) Chen[13] data of possibly disrupted flow measured at T_{in} = 297.9 K, $\dot{m}$ = 0.871 g·s^{-1}, ID = 1.5 mm.

in perfluoropropane. The experimental measurements of the throttling process of *n*-C_3F_8 performed and analyzed by us over a period of several years have revealed a significant negative effect of noncondensing gas impurities. A model of the perturbed-chain modification of statistical associating fluid theory (PC-SAFT)[10,11] and the Peng-Robinson cubic equation of state (PR EOS)[12] were employed for a theoretical description of the gas−liquid interaction and for estimating the Henry's law constant. The solubility was investigated at a low gas partial pressure of around 0.1 MPa.

Throttling Process of Gas-Contaminated Refrigerant

Evaporative cooling circuits, such as those for household refrigerators, deep freezers, air-conditioning units, and even special applications like the cooling systems of particle detectors, often use capillary tubes as expansion devices. Figure 1a shows the typical throttling profile of pressure (p) and saturation pressure (p_{sat}) calculated from the measured temperature along the capillary tube; z denotes distance from the capillary tube inlet. The data were measured with R134a by Huerta et al.[9] The plotted data are valid for the adiabatic case of a clean refrigerant flow commonly consisting of four separate regions: *one-phase flow of a subcooled liquid*, *one-phase flow of a superheated liquid*, *two-phase metastable flow*, and *thermodynamically equilibrated two-phase flow*.[7] Both of the inner flow regions are thermodynamically metastable since the superheated liquid phase persists at a lower pressure than the corresponding saturation pressure at the current refrigerant temperature.

The throttling process in the vapor cooling circuit is quite often affected by various negative effects. One of these may be the presence of noncondensing gases in the circuit refrigerant fill. The noncondensing gases usually accumulate in the condenser and increase the total condensing pressure due to their partial pressure. The observed increased pressure within the condenser is not the single effect of gas impurities. Since many refrigerants are relatively good solvents, the noncondensing gases dissolve in the liquid refrigerant circulating in the whole circuit.

The presence of contaminating gases also affects the conditions at the onset of vaporization, which can disrupt the refrigerant throttling process. The partial pressure of the noncondensing gases increases the total pressure inside the capillary tube, which causes the onset of vaporization to occur at a higher pressure, in fact closer to the capillary tube inlet. The single-phase flow becomes shorter, and consequently the refrigerant mass flow rate drops. Moreover, noncondensing gases cause the metastable region to vanish, and this phenomenon also reduces the mass flow.

Figure 1b summarizes our analysis of the experimental data of Chen and Lin,[13] measured using R134a under adiabatic conditions. No expected metastable region was recorded, and the vaporization, characteristic of successive temperature drop, started at a higher pressure than should normally correspond to the saturation pressure. Accordingly, our evaluation of Chen and Lin's data points to the probable presence of noncondensing gases inside the circuit.

Observations during Our Recent Experimental Test with n-C_3F_8. A special copper−nickel capillary tube equipped with a set of precise pressure transducers and temperature sensors of NTC, Pt1000, and Pt100 type was designed, manufactured, and afterward tested in our laboratory. A versatile testing vapor cooling circuit working with *n*-C_3F_8 refrigerant in a dry (fully oil-free) mode was used for our experimental tests. The operating conditions—refrigerant pressure and temperature at the capillary tube inlet and the evaporative pressure—were changed by a set of regulating valves (PR, pressure regulator; BPR, back pressure regulator), a PID controlled heater, heat exchangers with chilled water, and a subcooler. The capillary tube and the cooling circuit were similar to those described in our previous work.[2] The setup allowed detailed monitoring of the throttling process in the adiabatic capillary tube by mass flow rate measurements and through detecting the pressure and the relevant temperature profile along the capillary. The presence of noncondensing gases (in our case air) in the circuit was controlled by comparing the absolute pressure inside the condenser with the saturation pressure corresponding to the condenser temperature before each test.

An example of the clean refrigerant flow and the air-contaminated flow through the capillary tube is demonstrated in Figure 2. The flow conditions, i.e., inlet pressure and temperature, were similar in both cases. As shown in Figure 2b, we detected no metastable region and, similarly to the Chen and Lin data,[13] the two-phase flow started earlier than in the case of a clean refrigerant flow over the simulated runs. This

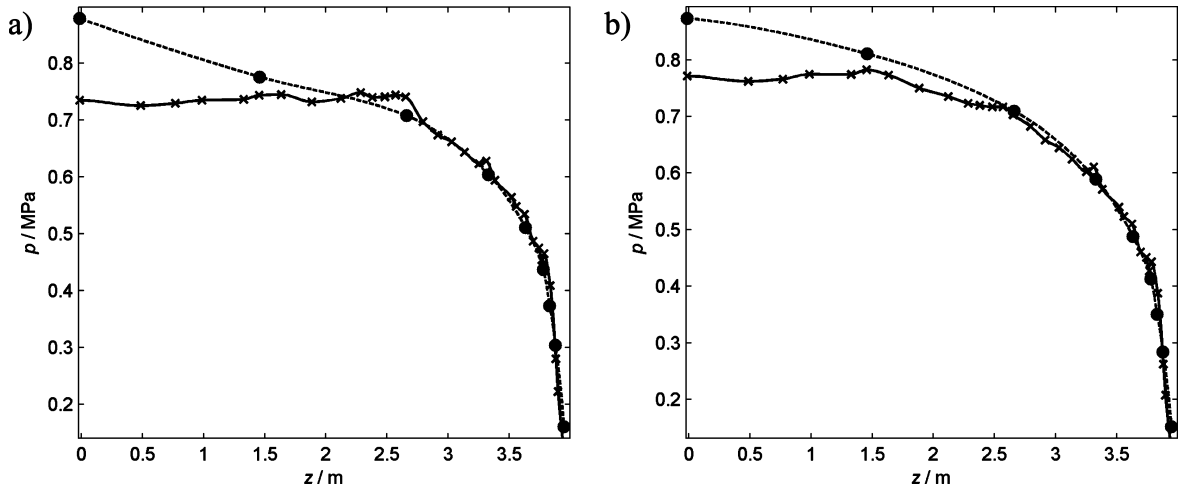

Figure 2. Comparison of: -●-, pressure; -×-, saturation pressure profiles measured in this study with R218 on capillary tube with ID = 0.95 mm for two cases with a low degree of subcooling and consequently low mass flow rate. (a) Capillary flow of pure refrigerant with quite significant metastable region: T_{in} = 292.6 K, $\dot{m}$ = 1.55 g·s^{-1}. (b) Flow of refrigerant contaminated by dissolved air with shifted saturation pressure and decreased mass flow rate, $\dot{m}$ = 1.35 g·s^{-1}. The inlet conditions p_{in} and T_{in} = 293.1 K were the same as in case a.

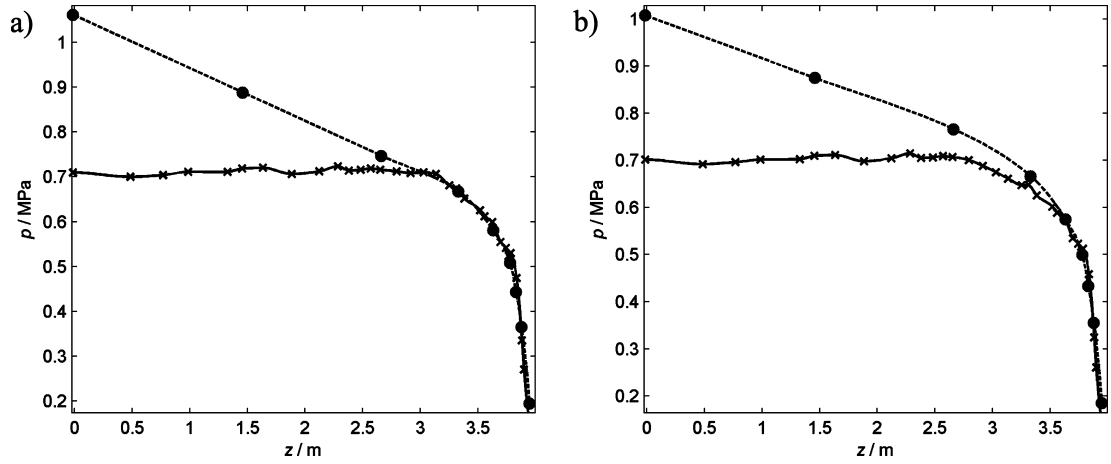

Figure 3. Comparison of: -●-, pressure; -×-, saturation pressure profiles measured in this study with R218, ID = 0.95 mm. Examples correspond to a high degree of subcooling and high mass flow rate compared to those shown in Figure 2. (a) Clean refrigerant flow at T_{in} = 291.4 K, $\dot{m}$ = 2.12 g·s^{-1}. (b) Flow of contaminated refrigerant at T_{in} = 291.0 K and decreased mass flow rate $\dot{m}$ = 1.85 g·s^{-1}.

resulted in a decrease of approximately 15 % in the refrigerant mass flow rate delivered through the capillary tube. The air contamination caused an increase of 0.010 MPa between the absolute pressure within the condenser and the saturation pressure corresponding to condensing temperature before the test run.

Another more transparent example is shown in Figure 3. The measured data were obtained with a high degree of subcooling, which results in the relatively short metastable region detectable in the clean refrigerant flow (Figure 3a). The pressure difference inside the condenser was 0.023 MPa in the case with contaminated refrigerant (Figure 3b). The vaporization process started at a pressure approximately 0.05 MPa higher than should correspond to the saturation pressure. The mass flow rate of the air-contaminated refrigerant was roughly 15 % lower than for the clean refrigerant flow analyses under the relevant capillary inlet and outlet conditions.

A numerical simulation of the saturated fluorocarbon refrigerant flow through the capillary tube, including the effect of gas impurities, is now being prepared. The success of the development of this extended model relies on knowledge of the temperature dependence of the Henry's law constant (k_H).

Henry's Law Constant of Saturated Fluorocarbons

Little experimental data on the solubility of gases in saturated fluorocarbons are available in the literature. Until now, most attention has been focused on oxygen since this gas is of interest for medical and environmental applications. However, the solubility of nitrogen and other gases, important for refrigerant gas-contamination modeling, has been investigated experimentally only sparsely. Therefore, a theoretical approach using an equation of state is vital for estimating the Henry's law constant. The temperature dependency of the Henry's law constant was predicted in this study by two different equations of state, PR EOS and PC-SAFT. A comparison of these two models should provide information about a representative Henry's law constant value for nitrogen, which is the major contaminator dissolved in n-C_3F_8 refrigerant.

PC-SAFT Parameters for Fluorocarbons. The PC-SAFT model uses a description of nonassociating molecules by three temperature-independent parameters: the number of segments per chain (m), the segment diameter (σ), and the segment energy parameter (ε/k_B), where k_B is the Boltzmann constant, k_B = 1.38065·10^{-23} J·K^{-1}. No such complete molecular parameters of saturated fluorocarbons for PC-SAFT have been

found in the literature. Therefore, the parameters m, σ, and ε/k_B had to be determined by fitting the vapor pressure (p) and the saturated liquid density (ρ_L) in a manner similar to that used by Gross and Sadowski[10] or by Dias et al.[14] The Levenberg−Marquardt algorithm was used to minimize the objective function given as

$$\sum_i^N \left(1 - \frac{p_{\mathrm{cal},i}}{p_{\mathrm{exp},i}}\right)^2 + \left(1 - \frac{\rho_{\mathrm{L,cal},i}}{\rho_{\mathrm{L,exp},i}}\right)^2 = \mathrm{MIN} \qquad (1)$$

where N is the number of fitted points; the subscript cal corresponds to PC-SAFT result, and the subscript exp to fitted saturation data.

Since PC-SAFT was to be employed for solubility calculation at temperatures close to room temperature, the molecular parameters were correlated only up to the maximum reduced temperature of 0.95. Table 1 summarizes the PC-SAFT parameters calculated for the gases considered here and for the fluorocarbon series from perfluoromethane (CF_4) to perfluorononane (n-C_9F_{20}). The temperature ranges covered by the data, obtained either from NIST[15] or from other experimental studies,[16−18] are also listed.

The average deviation (δ) and the standard deviation (s) were defined in the following manner

$$\delta = \frac{1}{N}\sum_i^N \frac{x_{\mathrm{exp},i} - x_{\mathrm{cal},i}}{x_{\mathrm{exp},i}} \qquad (2)$$

$$s = \sqrt{\frac{1}{N}\sum_i^N \left(\frac{x_{\mathrm{exp},i} - x_{\mathrm{cal},i}}{x_{\mathrm{exp},i}}\right)^2 - \delta^2} \qquad (3)$$

where general variable x is set either to vapor pressure (p) or to saturated liquid density (ρ_L).

The density of three fluoroinerts was measured using a density and sound analyzer (DSA 48 from Manufacturer AP Paar GmbH, Graz, Austria) in the indicated temperature ranges.

$$\begin{aligned} &n\text{-}C_6F_{14} \text{ for } T = (278 \text{ to } 308)\ \mathrm{K}: \\ &\rho/\mathrm{mol{\cdot}m^{-3}} = 7565.6\text{–}8.685{\cdot}T/\mathrm{K} \\ &n\text{-}C_7F_{16} \text{ for } T = (278 \text{ to } 308)\ \mathrm{K}: \\ &\rho/\mathrm{mol{\cdot}m^{-3}} = 6448.4\text{–}6.733{\cdot}T/\mathrm{K} \\ &n\text{-}C_8F_{18} \text{ for } T = (278 \text{ to } 308)\ \mathrm{K}: \\ &\rho/\mathrm{mol{\cdot}m^{-3}} = 5789.5\text{–}5.943{\cdot}T/\mathrm{K} \end{aligned} \qquad (4)$$

The liquid density of perfluoroheptane (n-C_7F_{16}), determined in our laboratory, was approximated by eq 4 in this study.

Figure 4 compares the saturation data for n-C_3F_8 taken from NIST and calculated by PC-SAFT in a $\log(pv)$ diagram.

The mixtures are investigated in PC-SAFT using the conventional Berthelot−Lorentz combining rules. The parameters between the pair segments are given as

$$\sigma_{ij} = \frac{1}{2}(\sigma_i + \sigma_j) \qquad (5)$$

$$\varepsilon_{ij} = \sqrt{\varepsilon_i \varepsilon_j}(1 - k_{ij}) \qquad (6)$$

where k_{ij} is the unknown binary interaction parameter that is to be defined on the premises of the available experimental data.

The choice of the gases for the study was determined by the gas expected to be ambient around the structures in our applications. Air ($N_2 + O_2$) and a pure N_2 atmosphere are likely to be the most frequent cases to contaminate n-C_3F_8. Xe, an inert gas with predictable solubility behavior and sufficient available experimental data, was taken as the reference.

Solubility of Oxygen in Fluorocarbons and Hydrocarbons. Since saturated fluorocarbons are good nontoxic solvents, they are used for example as oxygen carriers in blood substitution. Such a special and important application requires a detailed study of oxygen solubility in fluorinerts. Many researchers have performed detailed studies of oxygen solubility in fluorocarbons mostly consisting of six to nine carbons; see, e.g., studies of Gomes et al.[19] or Dias et al.[18,20,21] The solubility of oxygen in saturated fluorocarbons typically exhibits strong temperature dependency. Figure 5 shows the Henry's law constant of oxygen dissolved in four saturated fluorocarbons varying with a modified reduced temperature that we defined as

Table 1. Molar Mass M, Segment Number m, Segment Diameter σ, Segment Energy Parameter ε/k_B, Temperature Range of Fitted Data (T_{min} to T_{max}), Source of Fitted Data, Average Deviation δ, and Standard Deviation s of Vapor Pressure p and Liquid Density ρ_L for PC-SAFT

formula	M [g·mol^{-1}]	m [−]	σ [Å]	ε/k_B [K]	T_{min} [K]	T_{max} [K]	data source	$100\delta(p)$	$100\delta(\rho_L)$	$100s(p)$	$100s(\rho_L)$
O_2	31.999	1.0740	3.2598	117.729	73	147	15	0.132	−0.122	0.380	0.882
Xe	131.290	0.9147	4.0747	237.682	163	276	15	0.012	−0.008	0.310	0.491
N_2	28.013	1.2053	3.3130	90.960	63	126	[a]				
CF_4	88.004	2.2326	3.1050	120.998	128	216	15	0.073	−0.069	0.134	0.657
n-C_2F_6	138.012	2.8108	3.3128	140.512	175	279	15	0.030	−0.028	0.156	0.281
n-C_3F_8	188.019	3.2747	3.4579	155.080	196	328	15	0.036	−0.033	0.350	0.322
n-C_4F_{10}	238.027	3.7325	3.5567	164.583	225	367	15	0.095	−0.082	0.566	0.946
n-C_5F_{12}	288.034	4.3437	3.5851	169.208	253	400	15	0.054	−0.044	0.943	0.390
n-C_6F_{14}	338.042	4.8562	3.6440	173.414	288	333	16	0.003	−0.002	0.090	0.207
n-C_7F_{16}	388.049	5.4127	3.6739	176.403	278	333	17[b]	0.004	−0.003	0.078	0.376
n-C_8F_{18}	438.057	5.6756	3.7618	182.796	288	377	18	0.069	−0.009	2.383	0.478
n-C_9F_{20}	488.064	6.1774	3.7973	185.597	288	333	16	0.005	−0.001	0.581	0.084

[a] Parameters taken from Gross and Sadowski.[10] [b] Only vapor pressure.

$$T^* = \frac{T/\mathrm{K}}{(T_{C1}/\mathrm{K})^{M} \cdot (T_{C2}/\mathrm{K})^{1-M}} \quad (7)$$

where T_{C1} and T_{C2} denote critical temperature of the solvent and the solute, respectively. The use of T^*, instead of absolute temperature or solvent reduced temperature, provides the Henry's law constant dependency for all four analyzed fluorocarbons in the shape of a single curve. Exponent M in eq 7 has a value of 0.38. The experimental data plotted in Figure 5 are taken from studies by Dias et al.[18,20,21]

The Henry's law constant for oxygen dissolved in fluorocarbons containing from six to nine carbons is approximated within the temperature interval of Dias's experimental data, (287 to 313) K, by the following equation

$$k_H/\mathrm{MPa} = a_H + b_H(T^*)^{c_H} \quad (8)$$

In eq 8, the coefficients and the exponent were found to be: $a_H = 16.616$ MPa, $b_H = 0.060$ MPa, and $c_H = 19.200$.

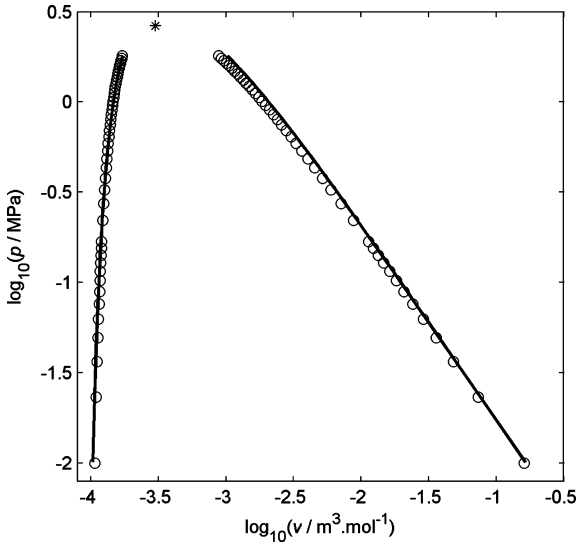

Figure 4. log(pv) diagram of n-C_3F_8: ○, NIST data;[15] −, PC-SAFT results; *, critical point.

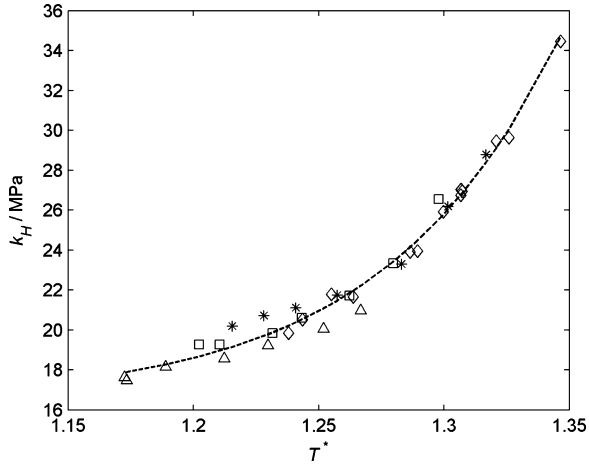

Figure 5. Henry's law constant k_H for oxygen and fluorocarbons as a function of dimensionless temperature T^*. Data taken from studies of Dias et al.:[18,20,21] ◇, n-C_6F_{14}; *, n-C_7F_{16}; □, n-C_8F_{18}; Δ, n-C_9F_{20}; --, correlation of Henry's law constant given by eq 8.

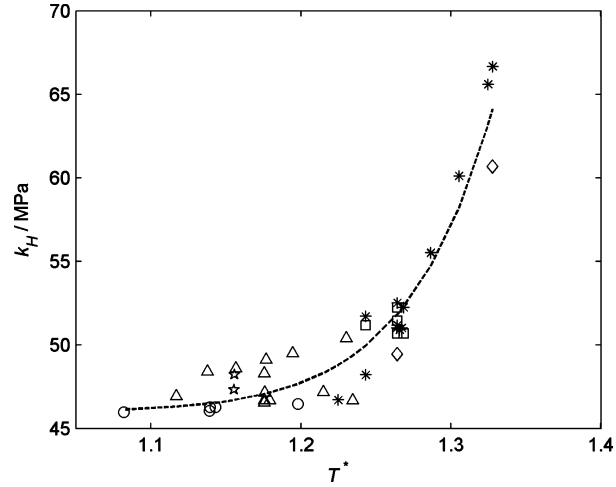

Figure 6. Henry's law constant k_H for oxygen and hydrocarbons as a function of dimensionless temperature T^*. Experimental data:[20,22−27] ◇, n-C_5H_{12}; *, n-C_6H_{14}; □, n-C_7H_{16}; Δ, n-C_8H_{18}; ☆, n-C_9H_{20}; ○, n-$C_{10}H_{22}$; --, correlation of Henry's law constant given by eq 8.

Equation 8 describing the Henry's law constant dependency was also tested on experimental data from the literature[20,22−27] for oxygen solubility in hydrocarbons, which have a number of carbons similar to the fluorocarbons considered in our study. Figure 6 shows the Henry's law constant of the oxygen dissolved in hydrocarbons dependent on modified reduced temperature.

Exponent M in eq 7 was set to 0.38 and had the same value as for fluorocarbons, while the applied coefficients and exponent values were as follows: $a_H = 45.961$ MPa, $b_H = 0.027$ MPa, and $c_H = 23.000$. Equation 8 provides a qualitatively sufficient description of the Henry's law constant for oxygen dissolved in hydrocarbons.

Both PC-SAFT and PR EOS were employed to predict the solubility of oxygen in fluorinert liquids. Figure 7 shows the temperature variation of the binary interaction parameter based on the experimental data of Dias et al.[18,20,21] Parameter k_{ij} for oxygen and fluorocarbons is a strongly temperature-dependent parameter for both EOSs. This fact restrains the usage of a universal constant value of k_{ij} for effective prediction of oxygen solubility in fluorinerts. This confirms the conclusion of Dias et al.[21] Figure 8a also shows that predictions by PC-SAFT and PR EOS, considering the constant binary interaction parameter k_{ij}, are quite similar. However, neither of the two EOSs provides fully comprehensive information about the temperature dependency of the Henry's law constant.

Discrepancy of predicted oxygen solubility is caused by additional association of organic fluorine compounds and oxygen as reported for instance by Buchachenko and Pokroskaya.[28] Pamies[29] and Dias et al.[14] successfully modeled the oxygen solubility with soft-SAFT by adding the cross-association energy term to the total Helmholtz free energy of the system. Both molecular oxygen and fluorocarbon could be considered as molecules with two equivalent associating sites on each. In this study, a similar approach to that introduced by Pamies[29] and Dias et al.[14] was employed on PC-SAFT. Contribution of the associating interactions was defined in terms of the Chapman et al.[30] and Huang and Radosz[31] models. The cross-association parameters were set constant for all four investigated mixtures. Values of the volume of interaction κ^{AB} and the association energy ε^{AB} were found to be $\kappa^{AB} = 0.00637$ and $\varepsilon^{AB} = 1586.5$ K. Binary interaction parameter k_{ij} for PC-SAFT including the cross-association term was determined to be: 0.462 for n-C_6F_{14}, 0.423 for n-C_7F_{16}, 0.401 for n-C_8F_{18}, and 0.374 for n-C_9F_{20}.

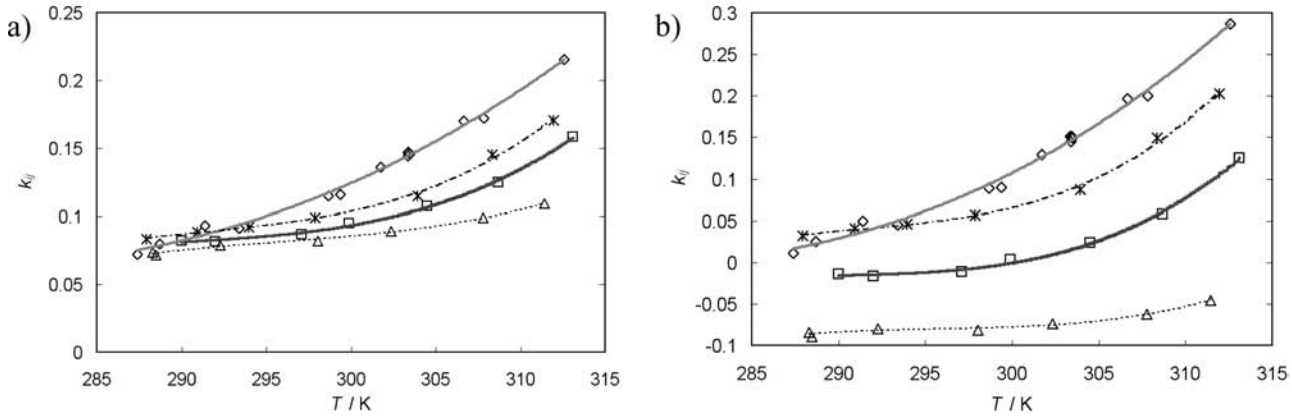

Figure 7. Binary interaction parameter k_{ij} determined from experimental data for oxygen dissolved in saturated fluorocarbons (a) for PC-SAFT and (b) for PR EOS. Experimental data:[18,20,21] ◇, n-C_6F_{14}; *, n-C_7F_{16}; □, n-C_8F_{18}; Δ, n-C_9F_{20}.

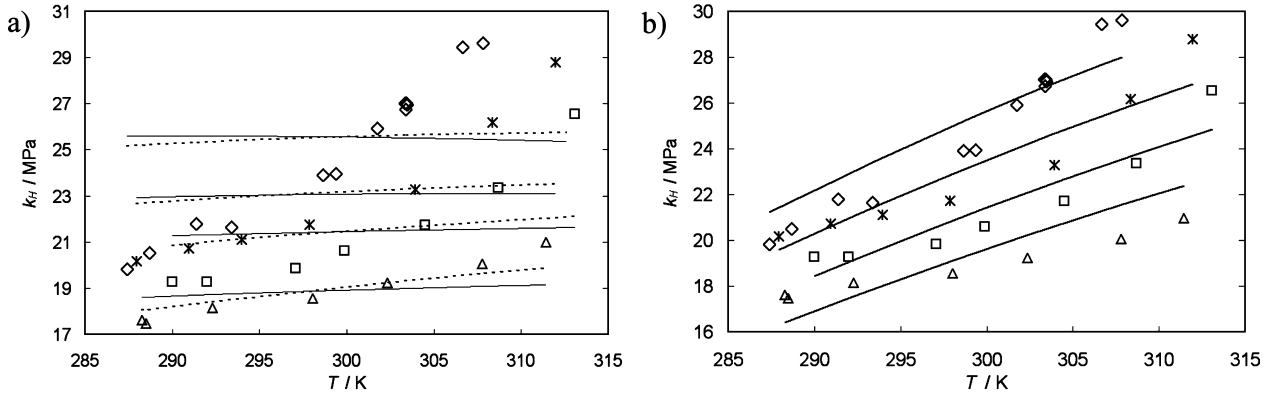

Figure 8. Henry's law constant k_H for oxygen and fluorocarbons. Comparison of experimental data,[18,20,21] ◇, n-C_6F_{14}; *, n-C_7F_{16}; □, n-C_8F_{18}; Δ, n-C_9F_{20}, with the predictions of: (a) −, PC-SAFT; --, PR EOS; (b) −, PC-SAFT with the cross-associating model using a constant binary interaction parameter k_{ij}.

Figure 8b compares experimental data of Dias et al.[18,20,21] with PC-SAFT including the cross-association model. The average relative deviation (ARD) of the predicted Henry's law constant and experimental data given by eq 9 was found to be 0.045.

$$\mathrm{ARD} = \frac{1}{N}\sum_{i=1}^{N} |k_{\mathrm{H,exp},i} - k_{\mathrm{H,cal},i}|/k_{\mathrm{H,exp},i} \qquad (9)$$

Solubility of Xenon. The solubility of an inert gas, namely, xenon, in saturated fluorocarbons was investigated as a reference case. Xenon interacts normally with the fluorinerts compared to oxygen. The temperature variation of the Henry's law constant for three commonly used fluorocarbons in our applications is demonstrated in Figure 9. The experimental data were taken from Dias et al.[14]

Exponent M in the definition of the modified reduced temperature (eq 7) was 0.28 in this case. The temperature dependency of the Henry's law constant was again correlated by eq 8, where the coefficients and the exponent of eq 8 have the following values: $a_H = -3.545$ MPa, $b_H = 10.908$ MPa, and $c_H = 1.680$.

Unlike in the case of oxygen solubility, the xenon solubility in saturated fluorocarbons can be successfully modeled both with PC-SAFT and with PR EOS, using a constant value of binary interaction parameter k_{ij}. The individual binary interaction parameters for xenon were found to be as follows in the case of PC-SAFT: 0.084 for n-C_6F_{14}, 0.086 for n-C_7F_{16}, and 0.081 for n-C_8F_{18}. Since the values of k_{ij} do not differ greatly from each other, an average k_{ij} value of 0.084 was successfully used for PC-SAFT prediction. Figure 10 compares the experimental data of Dias et al.[14] with the PC-SAFT results. The ARD was 0.018 when using the universal k_{ij} parameter. PC-SAFT interpreted the temperature dependency of the Henry's law constant for xenon quite accurately for all three fluorocarbons in the considered temperature interval between (278 and 325) K.

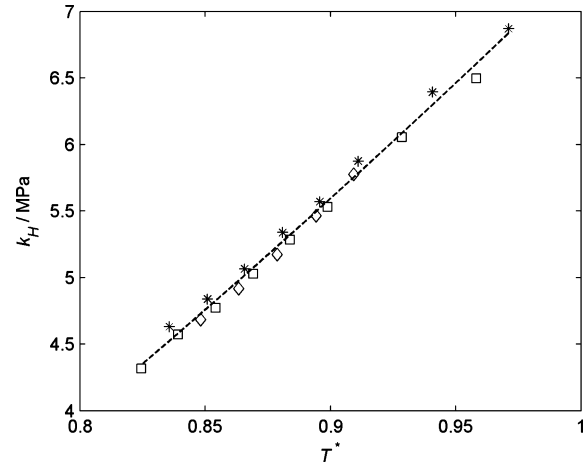

Figure 9. Henry's law constant for xenon and fluorocarbon dependence on dimensionless temperature T^*. Comparison of experimental data[14] and k_H correlation. ◇, n-C_6F_{14}; *, n-C_7F_{16}; □, n-C_8F_{18}; --, eq 8.

Figure 11a shows the results of PR EOS with k_{ij} parameters individually fitted for each fluorocarbon. Optimal values of k_{ij}

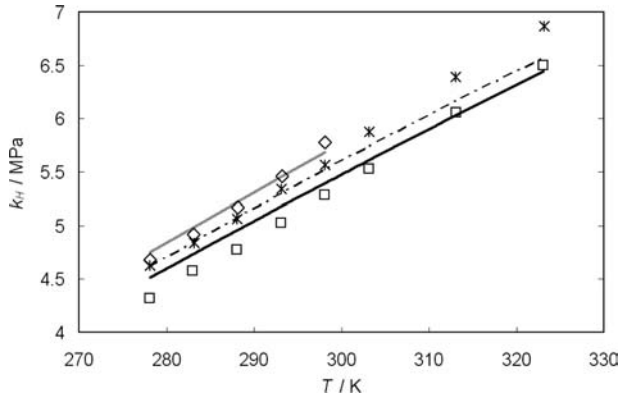

Figure 10. Comparison of the Henry's law constant k_H of xenon Experimental data[14] ◇, n-C_6F_{14}; *, n-C_7F_{16}; □, n-C_8F_{18}; versus the PC-SAFT prediction by considered universal k_{ij} parameter 0.084.

were found to be: 0.097 for n-C_6F_{14}, 0.095 for n-C_7F_{16}, and 0.076 for n-C_8F_{18}.

The prediction by PR EOS was also considered when applying the overall average value of binary interaction parameter $k_{ij} = 0.088$ (see Figure 11b). This approach resulted in a uniform Henry's law constant for all three fluorocarbons. This prediction is still in generally good agreement with the experimental data. A comparison between the ARD for the predicted Henry's law constant with the use of a single k_{ij} parameter and the experimental data showed a higher value (ARD = 0.039) for PR EOS than the PC-SAFT prediction (ARD = 0.018).

Solubility of Nitrogen. Unfortunately, very little data have been published on the solubility of nitrogen in saturated fluorocarbons. Nitrogen seems to have been less attractive than oxygen for studies of the major application of fluorocarbons as solvents or as gas carriers. However, nitrogen is the most important gas for contamination by noncondensing gases in fluorocarbons used as refrigerants. Refrigerants are very often contaminated by air, which can be approximately treated as pure nitrogen. We were able to trace only one set of experimental data for nitrogen solubility in saturated fluorocarbon, reflecting temperature dependency, which was presented by Gjaldbaek and Hildebrand.[32] The authors measured the temperature dependency of nitrogen solubility in n-C_7F_{16}.

Figure 12a shows the temperature dependency of a binary interaction parameter for nitrogen dissolved in n-C_7F_{16} evaluated for both PC-SAFT and PR EOS on the basis of the Gjaldbaek and Hilderbrand data.[32] The k_{ij} parameter remained almost constant in both cases. Its average value was derived to be 0.062 for PC-SAFT and −0.017 for PR EOS. The almost uniform k_{ij} parameter points to normal interaction of nitrogen with fluorocarbons, so the nitrogen solubility seems to be similar to xenon without additional association. Oxygen shows a typical strong temperature dependence of the k_{ij} parameter (see for comparison also Figure 7).

Figure 12b shows the Henry's law constant for N_2 and n-C_7F_{16} determined experimentally by Gjaldbaek and Hilderbrand[32] in comparison to predictions via PC-SAFT and PR EOS in the range of operating conditions between (250 and 330) K. However, it is hard to say which type of prediction might be closer to the real solubility of N_2 in n-C_7F_{16}. It is essential to note that the experimental data are quite limited and can only serve for an approximate prediction of k_{ij}.

In addition, the Henry's law constant was also predicted by both EOSs, for the simplified case with the binary interaction parameters k_{ij} set to zero (see in Figure 12b). Setting up the parameter $k_{ij} = 0$ resulted in an almost negligible difference in the predicted Henry's law constant in the case of PR EOS. The PC-SAFT is slightly more sensitive to the k_{ij} definition. For example, setting k_{ij} equal to zero lowered the predicted Henry's law constant by 30 %.

An invariable binary interaction parameter for N_2 and n-C_7F_{16} together with its low absolute values for both EOSs allowed us to assume that we may consider a uniform k_{ij} parameter also for a mixture of N_2 and n-C_3F_8, which was in fact our target fluid.

Figure 13 shows the temperature dependency of the Henry's law constant for N_2 and n-C_3F_8 predicted by both EOSs, in both cases setting the k_{ij} parameter equal to its average values evaluated for n-C_7F_{16} and for the simplified instance with k_{ij} set to zero. The two EOSs provided quite similar Henry's law constants for parameters $k_{ij} = 0$. The ARD between the results of PC-SAFT and PR EOS with nonzero k_{ij} parameters is approximately 0.14 within the considered temperature range of (240 and 320) K. We can conclude from Figure 13 that the relevant Henry's law constant value can fall in the area between the curves corresponding to PC-SAFT results with $k_{ij} = 0.062$ and $k_{ij} = 0$.

The Henry's law constants of nitrogen dissolved in n-C_3F_8 and n-C_7F_{16} predicted by both PC-SAFT and PR EOS were subsequently treated using Krause and Benson's[33] three-parameter correlation of the following form

$$\ln(k_H\,[\mathrm{MPa}]) = a + b\frac{(1 - T_r)^{1/3}}{T_r^2} + c\frac{(1 - T_r)^{2/3}}{T_r^2} \quad (10)$$

In eq 10, T_r represents the reduced temperature of the solvent. Parameters a, b, and c, listed in Table 2, were determined from predictions via both EOSs with $k_{ij} = -0.017$ in the case of PR EOS and $k_{ij} = 0.062$ in the case of PC-SAFT. The relevant temperature ranges were (240 to 320) K for n-C_3F_8 and (230 to 370) K for n-C_7F_{16}.

Equation 10 with the parameters presented in Table 2 represents two final predictions of the Henry's law constant for nitrogen dissolved either in n-C_3F_8 or in n-C_7F_{16}. The deficiency of available experimental data for comparison with modeled predictions made it impossible to evaluate strictly and explicitly which EOS would give a better prediction of the nitrogen solubility in saturated fluorocarbons. The Henry's law constant correlations derived both from PC-SAFT and from PR EOS might therefore be considered at this point.

Conclusion

The available solubility experimental data for oxygen, xenon, and nitrogen dissolved in saturated fluorocarbons were collected from the literature, then analyzed and used to describe the Henry's law constant temperature dependency at low gas partial pressure around 0.1 MPa. A simple Henry's law constant correlation for oxygen and xenon was derived employing a combined reduced temperature. The cubic Peng-Robinson (PR) equation of state (EOS) and perturbed-chain statistical associating fluid theory (PC-SAFT) were used for predicting gas solubility in fluorocarbons. The oxygen solubility was found to be strongly temperature dependent as reflected on the binary interaction parameter. This fact indicates association of oxygen and saturated fluorocarbons as reported previously in the literature. Both EOSs in standard form provide only a rough description of the temperature dependency of the oxygen

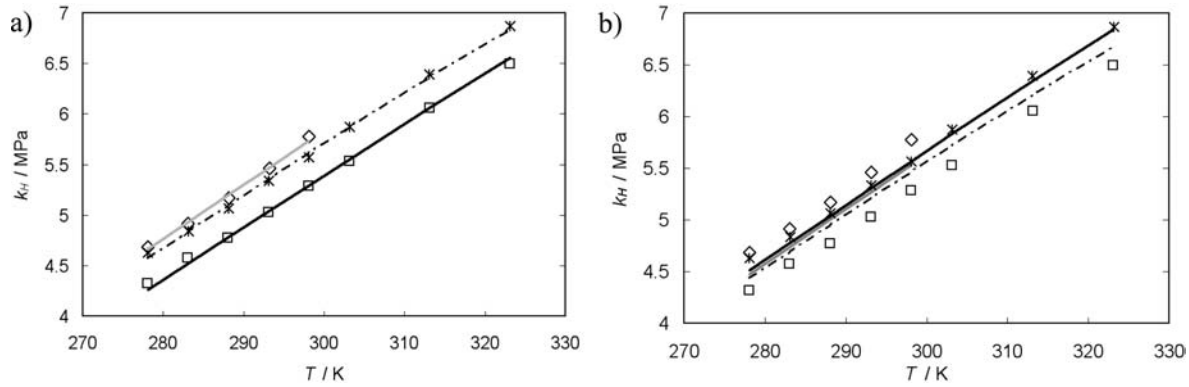

Figure 11. Henry's law constant for xenon and fluorocarbons. Comparison of experimental data[14] ◇, *n*-C_6F_{14}; *, *n*-C_7F_{16}; □, *n*-C_8F_{18}; and PR EOS prediction (a) with individual k_{ij} parameters 0.097 for *n*-C_6F_{14}, 0.095 for *n*-C_7F_{16}, and 0.076 for *n*-C_8F_{18}; (b) with a universal $k_{ij} = 0.088$.

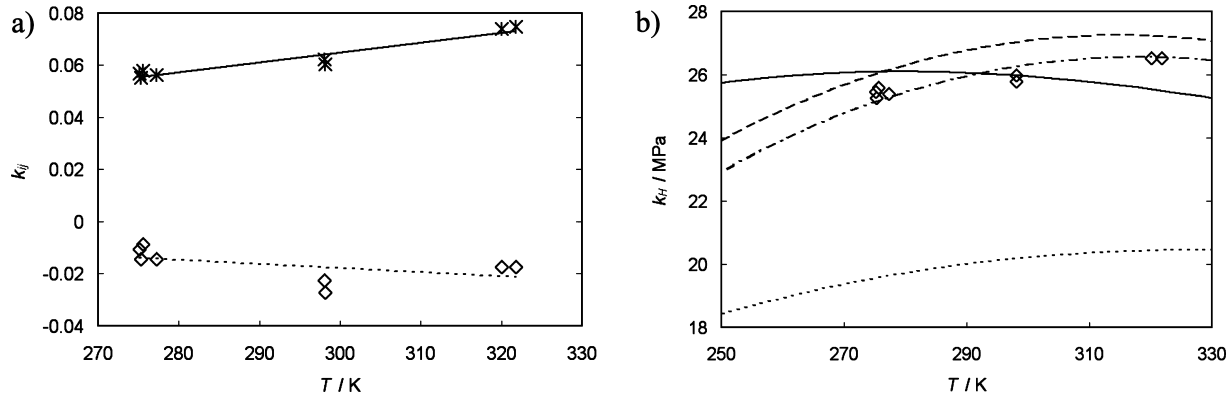

Figure 12. (a) Binary interaction parameter for N_2 and *n*-C_7F_{16}: *, PC-SAFT; ◇, PR EOS. (b) Henry's law constant for N_2 and *n*-C_7F_{16}. Comparison of experimental data,[32] ◇, and the predictions with different k_{ij} parameter: PC-SAFT, —, $k_{ij} = 0.062$; •••, $k_{ij} = 0.0$; and PR EOS, •-, $k_{ij} = -0.017$; --, $k_{ij} = 0.0$.

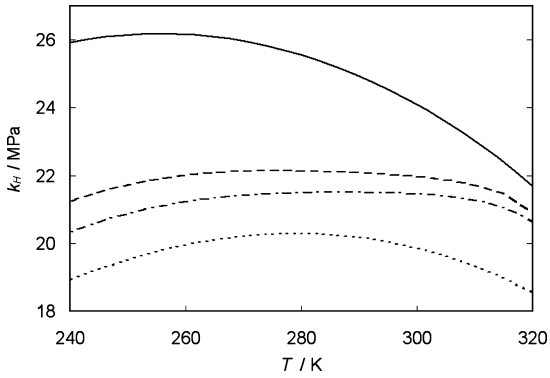

Figure 13. Predicted Henry's law constant for N_2 and *n*-C_3F_8. PC-SAFT, —, $k_{ij} = 0.062$; •••, $k_{ij} = 0.0$; and PR EOS, •-, $k_{ij} = -0.017$; --, $k_{ij} = 0.0$.

Table 2. Parameters *a*, *b*, and *c* in Benson and Krause's[33] Correlation 10 of the Henry's Law Constant for Nitrogen and Fluorocarbons

		a	*b*	*c*
n-C_3F_8	PR EOS	2.484	2.352	−2.929
	PC-SAFT	1.872	4.896	−5.798
n-C_7F_{16}	PR EOS	1.824	4.635	−5.347
	PC-SAFT	2.181	3.089	−3.475

solubility in fluorocarbons. On the other hand, PC-SAFT with a cross-associating model predicts oxygen solubility quite well. Next to oxygen solubility, both EOSs employed here can be successfully used for predicting the solubility of xenon and nitrogen in fluorocarbons. PC-SAFT predicts xenon solubility well with a universal binary interaction parameter $k_{ij} = 0.084$. The average relative deviation between the predicted Henry's law constant and the experimental data was less than ARD = 0.018.

The nitrogen solubility in perfluoropropane (*n*-C_3F_8) was correlated by both PC-SAFT and PR EOS using the binary interaction parameters $k_{ij} = 0.062$ and $k_{ij} = -0.017$, respectively. The binary interaction parameters were determined from experimental data for nitrogen solubility in perfluoroheptane (*n*-C_7F_{16}). The temperature correlations of the Henry's law constant were derived from the predicted data for nitrogen dissolved in *n*-C_3F_8 and in *n*-C_7F_{16} in the form of the Krause and Benson relation.

Temporary activity focuses on a theoretical solution of the problem of the disrupted throttling process of the *n*-C_3F_8 refrigerant contaminated by noncondensing gases. The evaluated Henry's law constant will be implemented into a numerical model of the two-phase flow of the refrigerant with dissolved gas impurities. Further analysis of our available experimental data collected during measurements verifying the flow behavior in capillary tubes with *n*-C_3F_8 refrigerant may reveal which Henry's law constant correlation is more relevant.

Acknowledgment

The authors are grateful to the CERN research centre in Geneva, where most of the experimental tests on the throttling process of gas-contaminated refrigerant were performed. Many thanks go to Mr. Jan Hrubý, from the Institute of Thermomechanics of AS ČR, for his remarkable help in estimating the Henry's law constant and also to Mr. Martin Lísal, from the Institute of Chemical Process Fundamentals of AS ČR, for his welcome advice on PC-SAFT.

Literature Cited

(1) Vacek, V.; Hallewel, G.; Ilie, S.; Lindsay, S. Perfluorocarbons and their Use in Cooling Systems for Semiconductor Particle Detectors. *Fluid Phase Equilib.* **2000**, *174*, 191–201.

(2) Vacek, V.; Vins, V. A Study of the Flow through Capillary Tubes Tuned for a Cooling Circuit with Saturated Fluorocarbon Refrigerants. *Int. J. Thermophys.* **2007**, *28*, 1490–1508.

(3) Olcese, M.; Rossi, L. P.; McMahon, S. J.; Vacek, V.; Bates, R. L.; Bonneau, P.; Doubrava, M.; Battistin, M.; Berry, S.; Pernegger, H.; Galuska, M.; Gorski, B.; et al. The Evaporative Cooling System for the ATLAS Inner Detector. *J. Instrumentation* **2008**, *3*, P07003.

(4) Gorski, B.; Bates, R. L.; Olcese, M.; Vacek, V. The Design and Prototyping of the ATLAS Inner Detector Evaporative Cooling SystemNuclear Science Symposium Conference Record 2, 16−22 Oct. 2004, IEEE, 677−681.

(5) Wong, T. N.; Ooi, K. T. Adiabatic Capillary Tube Expansion Devices: A Comparison of the Homogeneous Flow and the Separated Flow Models. *Appl. Therm. Eng.* **1996**, *16* (7), 625–634.

(6) Sami, S. M.; Tribes, C. Numerical Prediction of Capillary Tube Behavior with Pure and Binary Alternative Refrigerants. *Appl. Therm. Eng.* **1998**, *18* (6), 491–502.

(7) García-Valladares, O.; Pérez-Segarra, C. D.; Oliva, A. Numerical Simulation of Capillary Tube Expansion Devices Behavior with Pure and Mixed Refrigerants Considering Meta-Stable Region. *Appl. Therm. Eng.* **2002**, *22*, 173–182.

(8) Xu, B.; Bansal, P. K. Non-Adiabatic Capillary Tube Flow: a Homogeneous Model and Process Description. *Appl. Therm. Eng.* **2002**, *22*, 1801–1819.

(9) Huerta, A. A. S.; Fiorelli, F. A. S.; Silvares, O. M. Metastable Flow in Capillary Tubes: An Experimental Evaluation. *Exp. Therm. Fluid Sci.* **2007**, *31* (8), 957–966.

(10) Gross, J.; Sadowski, G. Perturbed-Chain SAFT: An Equation of State Based on a Perturbation Theory for Chain Molecules. *Ind. Eng. Chem. Res.* **2001**, *40*, 1244–1260.

(11) Gross, J.; Sadowski, G. Application of the Perturbed-Chain SAFT Equation of State to Associating Systems. *Ind. Eng. Chem. Res.* **2002**, *41*, 5510–5515.

(12) Peng, D. Y.; Robinson, D. B. New 2-Constant Equation of State. *Ind. Eng. Chem. Fundam.* **1976**, *15*, 59–64.

(13) Chen, D.; Lin, S. Underpressure of Vaporization of Refrigerant R-134a through a Diabatic Capillary Tube. *Int. J. Refrig.* **2001**, *24*, 261–271.

(14) Dias, A. M. A.; Pamies, J. C.; Coutinho, J. A. P.; Marrucho, I. M.; Vega, L. F. SAFT Modeling of the Solubility of Gases in Per-Fluoralkanes. *J. Phys. Chem. B* **2004**, *108*, 1450–1457.

(15) NIST WebBook Chemistry, June 2005, http://webbook.nist.gov/chemistry/.

(16) Dias, A. M. A.; Goncalves, C. M. B.; Caco, A. I.; Santos, L. M. N. B. F.; Pineiro, M. M.; Vega, L. F.; Coutinho, J. A. P.; Marrucho, I. Densities and Vapor Pressures of High Fluorinerted Compounds. *J. Chem. Eng. Data* **2005**, *50*, 1328–1333.

(17) Reid, R. C.; Prausnitz, J. M.; Polling, B. E. *The Properties of Gases and Liquids*, 4th ed.; McGraw-Hill Int. Editions: New York, 1988.

(18) Dias, A. M. A.; Caco, A. I.; Coutinho, J. A. P. Thermodynamic Properties of Perfluoro-n-Octane. *Fluid Phase Equilib.* **2004**, *225*, 39–47.

(19) Gomes, M. F. C.; Deschamps, J.; Menz, D.-H. Solubility of Dioxygen in Seven Fluorinated Liquids. *J. Fluorine Chem.* **2004**, *125*, 1325–1329.

(20) Dias, A. M. A.; Bonifa'cio, R. P.; Marrucho, I. M.; et al. Solubility of Oxygen in n-Hexane and in n-Perfluorohexane. Experimental Determination and Prediction by Molecular Simulation. *Phys. Chem. Chem. Phys.* **2003**, *5*, 543–549.

(21) Dias, A. M. A.; Freire, M.; Coutinho, J. A. P.; Marrucho, I. M. Solubility of Oxygen in Liquid Perfluorcarbons. *Fluid Phase Equilib.* **2004**, *222*, 325–330.

(22) Makranczy, J.; Megyery-Balog, K.; Rusz, L.; Patyi, L. Solubility of Gases in Normal-Alkanes. *Hung. J. Ind. Chem.* **1976**, *4*, 269–280.

(23) Guerry, D. Ph.D. thesis; Vanderbilt University, Nashville, TN, 1944.

(24) Thomsen, E. S.; Gjaldbaek, J. C. Solubility of Hydrogen, Nitrogen, Oxygen and Ethane in Normal Hydrocarbons. *Acta Chem. Scand.* **1963**, *17*, 127–133.

(25) Wilcock, R. J.; Battino, R.; Danforth, W. F. Solubilities of Gases in Liquids. 2. Solubilities of He, Ne, Ar, Kr, O_2, N_2, CO, CO_2, CH_4, CF_4 and SF_6 in Normal-Octane 1-Octanol, Normal-Decane, and 1-Decanol. *J. Chem. Thermodyn.* **1978**, *10*, 817–822.

(26) Cibulka, I.; Heintz, A. Partial Molar Volumes of Air-Component Gases in Binary Liquid Mixtures with n-Alkanes and 1-Alkanols at 298.15 K. *Fluid Phase Equilib.* **1995**, *107*, 235–255.

(27) Gomes, M. F. C.; Deschamps, J.; Padua, A. A. H. Effect of Bromine Substitution on the Solubility of Gases in Hydrocarbons and Fluorcarbons. *Fluid Phase Equilib.* **2007**, *251*, 128–136.

(28) Buchachenko, A. L.; Pokroskaya, M. Yu. Complexation of Molecular Oxygen with Organic Fluorine-Containing Molecules. *Russ. Chem. Bull.* **1984**, *33*, 2451–2454.

(29) Pamies, J. C. Bulk and Interfacial Properties of Chain Fluids: A Molecular Modelling Approach. PhD thesis, Universitat Rovira i Virgili, Tarragona, Spain, 2003.

(30) Chapman, W. G.; Gubbins, K. E.; Jackson, G.; Radosz, M. New Reference Equation of State for Associating Liquids. *Ind. Eng. Chem. Res.* **1990**, *29*, 1709–1721.

(31) Huang, S. H.; Radosz, M. Equation of State for Small, Large, Polydisperse, and Associating Molecules. *Ind. Eng. Chem. Res.* **1990**, *29*, 2284–2294.

(32) Gjaldbaek, J. C.; Hildebrand, J. H. The Solubility of Nitrogen in Carbon Disulfide, Benzene, Normal-Hexane and Cyclo-Hexane, and in 3 Fluorocarbons. *J. Am. Chem. Soc.* **1949**, *71*, 3147–3150.

(33) Krause, D.; Benson, B. B. The Solubility and Isotopic Fractionation of Gases in Dilute Aqueous Solution. IIa. Solubilities of the Noble Gases. *J. Solution Chem.* **1989**, *18*, 823–872.

Received for review November 3, 2008. Accepted January 21, 2009. The project has been supported by grants of the Ministry of Education, Youth and Sports of the Czech Republic: No.: LA08015 (cooperation with CERN), LA08032 (ATLAS-CERN), CAS IAA400720710, and by the Research Plan of the Institute of Thermomechanics AS ČR, vvi No. AV0Z20760514.

JE800819H